Journal of Zhejiang University-SCIENCE A (Applied Physics & Engineering)
ISSN 1673-565X (Print); ISSN 1862-1775 (Online)
www.zju.edu.cn/jzus; www.springerlink.com
E-mail: jzus@zju.edu.cn

# Probability-based method using RFEM for predicting wall deflection caused by excavation*

Yu-geng TANG
(*Department of Architecture, Hwa-Hsia Institute of Technology, Taiwan 23568, Taipei*)
E-mail: tang@cc.hwh.edu.tw

Received Jan. 20, 2011; Revision accepted May 20, 2011; Crosschecked Sept. 7, 2011

**Abstract:** This study employs the random finite element method (RFEM) to analyze the wall deflection caused by excavation. The RFEM combined random fields of material properties with the FEM through the Monte Carlo simulation. A well-documented excavation case history is employed to evaluate the influence of uncertainty of analysis parameters. This study shows that RFEM can provide reasonable estimations of the exceedance probability of wall deflection caused by excavation, and has the potential to be a useful tool to account for the uncertainties of material and model parameters in the numerical analysis.

**Key words:** Excavation, Random finite element method (RFEM), Uncertainty, Wall deflection
**doi:**10.1631/jzus.A1100016 **Document code:** A **CLC number:** TU476+.3

## 1 Introduction

Deep excavation to maximize the use of underground space is usually adopted to construct high-rise buildings in urban areas. To construct a deep basement, a deep retaining wall together with an appropriate bracing system must be designed first. For a deep excavation case, as illustrated in Fig. 1, ground movements are inevitable due to the relaxation of stresses during the deflection of the retaining wall (Schuster *et al.*, 2009). As the retaining wall deflects laterally toward the excavation zone, the ground behind the wall will move accordingly (Fig. 1). The vertical and lateral ground movements may cause the distortion of buildings adjacent to the excavation. As the building distorts and larger strains develop, the damage to the building may be observed. Therefore, the prevention of damage to adjacent buildings is recognized as one of the crucial tasks in the design of a deep braced excavation in urban area. This task may be achieved through the prediction of excavation-induced wall and ground movements, with which the potential of damage to adjacent buildings can be estimated. In practice, the settlement profile can be estimated using the simplified method (Kung *et al.*, 2007b) or the numerical methods (Kung *et al.*, 2007a; 2009). The engineer often adopts the magnitude of wall deflection as an indicator to evaluate the potential of damage to a building. Hence, this study focuses on the prediction of wall deflection caused by excavation.

## 2 Random finite element method

The random finite element method (RFEM) can be used to conduct the probabilistic analysis for estimating the probability of wall deflection. The crucial characteristic of the RFEM is that the uncertainty of input parameters, including the soil and nonsoil parameters, can be adequately addressed in the finite element analysis. Over the past decade, the RFEM has been employed to study the effects of uncertainty of soil properties on various geotechnical problems

* Project (No. NSC 99-2221-E-146-004) supported by the National Science Council

(Griffiths and Fenton, 2001; 2004; Fenton and Griffiths, 2002; Fenton *et al.*, 2005). In this study, the procedure of excavation analysis using the RFEM is developed and used to perform the probabilistic analysis of excavation-induced deformation.

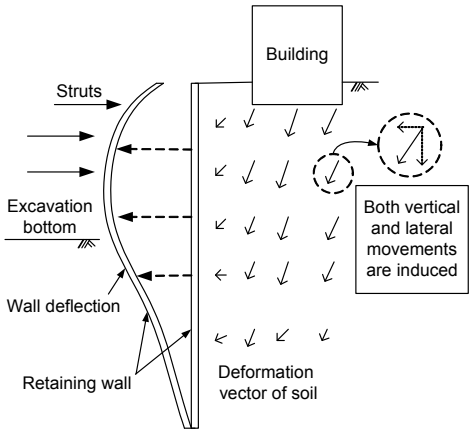


**Fig. 1 Schematic diagram of excavation effects (modified from Schuster *et al.* (2009))**

## 2.1 Framework of the RFEM

The analytical procedure of RFEM for deformation caused by excavation is shown in Fig. 2. This procedure incorporated the concept of random fields of material properties and the Monte Carlo simulation into the conventional FEM to form the RFEM. When using the developed RFEM procedure to analyze the excavation-induced wall deflection, the pattern of probability distribution of parameters and the number of simulations ($N_{\text{sim}}$) must be determined firstly. Secondly, the mean and standard deviation of selected random variables have to be determined. Then the analysis of excavation-induced wall deflection can be conducted using the Monte Carlo simulation through randomly generating a field of selected material parameters based on assigned probability distribution, mean, and standard deviation.

After repeatedly conducting the FEM analysis and the number of simulations $N_{\text{sim}}$ reaching the given number, the program will be terminated automatically and the results (e.g., the maximum wall deflection) are outputted and analyzed. Finally, according to the analysis results, the relative frequency and probability of the maximum wall deflection can be obtained for further judging the feasibility of excavation design.

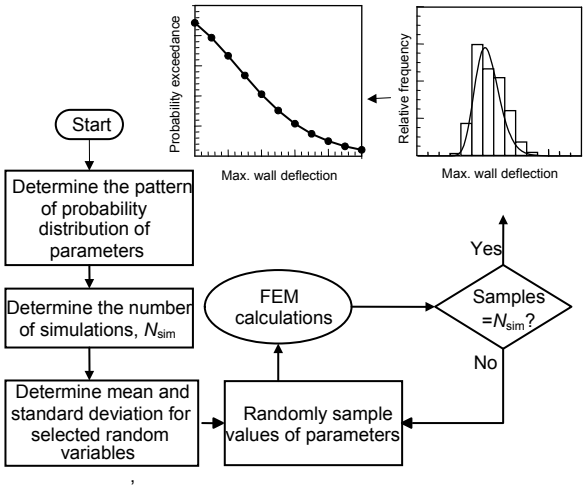


**Fig. 2 Procedure of the excavation analysis using the random finite element method**

## 2.2 Random variables generator

According to the procedure of proposed REFM in this study, the first task is to generate random variables with a specified joint probability distribution. Initially, the multiplicative linear congruential generator method (Barry, 1996; Honjo, 2008) is used to generate a sequence of integers. Specifically, the recursive formula used has the following format:

$$I_{j+1} = aI_j \,(\text{mod}\, m), \tag{1}$$

where $m$ is the modulus, and $a$ is positive integer called the multiplier. Eq. (1) will eventually repeat itself, with a period that is obviously not greater than $m$. If $a$ and $m$ are properly chosen, then the period will be of maximal length. The real uniform number between 0 and 1 that is returned is generally $I_{j+1}/m$. To satisfy the condition for generating a great number of random numbers, values of $a$=62 089 911 and $m=2^{31}-1$ proposed by Barry (1996) are adopted in this study. Thus, Eq. (1) has a full period of length, equal to $(2^{31}-1)-1$=2 147 483 646, i.e., the cycle of random numbers repeats after more than two billion trials. If standard normal random variables are required, the use of the Box-Muller transform method (Box and Muller, 1958) can produce a pair of Gaussian random numbers from a pair of uniform numbers. The equations of the Box-Muller transform method are

$$x_1 = \sqrt{-2\ln(U_1)}\cos(2\pi U_2),$$
$$x_2 = \sqrt{-2\ln(U_1)}\sin(2\pi U_2), \tag{2}$$

where $x_1$ and $x_2$ are a pair of normally distributed deviate with zero mean and unit variance. $U_1$ and $U_2$ are a pair of uniform random numbers generate from Eq. (1). Because the algorithm produces two random numbers at each time, it is common for the generation function to return the first value to the user, and cache the other value for returning on the next function call. In the case of lognormal random variables, the normal variables can be changed to generate lognormal variables by the following formulas:

$$\sigma_x^2 = \ln\left(\frac{\sigma_y^2}{\mu_y^2}+1\right),$$
$$\mu_x = \ln\mu_y - \frac{\sigma_x^2}{2}, \tag{3}$$
$$y = \mathrm{e}^x,$$

where $x$ and $y$ represent normal and lognormal variables, respectively, and $\mu$ and $\sigma$ are mean value and standard deviation, respectively.

## 3 Analysis of wall deflection using RFEM

### 3.1 Excavation case history

In this study, a quality excavation case history, the Formosa case (Ou *et al.*, 1993), is analyzed using the developed RFEM. This case is located in the Taipei basin and its foundation was constructed using the bottom-up construction method. A diaphragm wall, 0.8 m thick and 31 m deep, was used as the retaining wall. The maximum excavation depth was 18.45 m. The construction activities include seven stages of excavation and six stages of steel strut installation. Table 1 summarizes propping arrangements for the excavation case history and stiffness of struts. The stratigraphy of the Formosa case mostly consists of soft to medium clay. The depth at the top of the Chingmei Gravel Formation is roughly equal to 31 m. The stratigraphy and detailed construction activities are shown in Fig. 3.

**Table 1 Propping arrangements for the excavation case history and stiffness of struts**

| Stage | $H_e$ (m) | $H_p$ (m) | $k$ (kN/m$^2$) |
|---|---|---|---|
| 1 | 1.5 | – | – |
| 2 | 4.3 | 1.0 | 43400 |
| 3 | 6.9 | 3.7 | 50680 |
| 4 | 10.2 | 6.2 | 63740 |
| 5 | 13.2 | 9.5 | 101360 |
| 6 | 16.2 | 12.5 | 127480 |
| 7 | 18.45 | 15.5 | 127480 |

$H_e$ is the excavation depth; $H_p$ is the depth where the strut installed; and $k$ is the corresponding stiffness

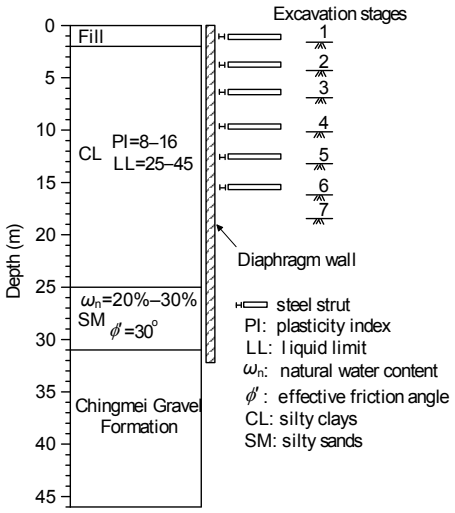


**Fig. 3 Stratigraphy and construction sequences of the Formosa case**

### 3.2 Soil models

The hyperbolic model (Duncan and Chang, 1970) was used to describe the sandy layers. The stress-strain characteristics of soils can be expressed as hyperbola:

$$\sigma_1 - \sigma_3 = \frac{\varepsilon}{\dfrac{1}{E_i} + \dfrac{\varepsilon}{(\sigma_1-\sigma_3)_{ult}}}, \tag{4}$$

where $\sigma_1$ is the maximum principal stress, $\sigma_3$ is the minimum principal stress, $\varepsilon$ is the axial strain, $E_i$ is the initial tangent modulus of the stress-strain curve, and $(\sigma_1-\sigma_3)_{ult}$ is the ultimate deviatoric stress.

The ultimate deviatoric stress can be determined by

$$(\sigma_1-\sigma_3)_{ult}=(\sigma_1-\sigma_3)_f/R_f, \tag{5}$$

where $R_f$ is the failure ratio and $(\sigma_1-\sigma_3)_f$ is the deviatoric stress at failure. Note that $R_f\leq 1.0$ and $R_f$=0.5–0.9 for most soils. The deviatoric stress at failure can be determined by

$$(\sigma_1-\sigma_3)_f=\frac{2c\cos\phi+2\sigma_3\sin\phi}{1-\sin\phi}, \tag{6}$$

where $c$ is the soil cohesion and $\phi$ is the soil friction angle. The stress level is defined as

$$\mathrm{SL}=\frac{\sigma_1-\sigma_3}{(\sigma_1-\sigma_3)_f}, \tag{7}$$

The initial stiffness modulus $E_i$ can be calculated by

$$E_i=KP_a\left(\frac{\sigma_3}{P_a}\right)^n, \tag{8}$$

where $P_a$ is the atmospheric pressure (=101.4 kPa), $K$ is the modulus number, and $n$ is the exponent of the elastic modulus.

The tangential modulus of soil $E_t$ can be obtained:

$$E_t=\left[1-\frac{R_f(1-\sin\phi)(\sigma_1-\sigma_3)}{2c\cos\phi+2\sigma_3\sin\phi}\right]^2 KP_a\left(\frac{\sigma_3}{P_a}\right)^n. \tag{9}$$

By incorporating Eqs. (6)–(8) into Eq. (9), the tangent modulus $E_t$ can be expressed as

$$E_t=E_i(1-R_f\mathrm{SL})^2, \tag{10}$$

Finally, the unloading-reloading stiffness modulus of soils can be calculated by

$$E_{ur}=K_{ur}P_a\left(\frac{\sigma_3}{P_a}\right)^n, \tag{11}$$

where $K_{ur}$ is the modulus number of soils during the unloading-reloading stages. A total of seven parameters, i.e., $c$, $\phi$, $n$, $K$, $K_{ur}$, $R_f$, and Poisson's ratio $\nu$, are required for the hyperbolic model to fully describe the stress-strain behavior of sand.

The pseudo plastic model (Hsieh and Ou, 1997) is employed in this study to describe the undrained stress-strain behavior of clayey soil. The clayey soil was assumed to behave as a nonlinear pseudo plastic material, which is characterized by a hyperbolic curve (Kondner and Zelasko, 1963):

$$\sigma_v-\sigma_h=\varepsilon/(a+b\varepsilon), \tag{12}$$

where $\sigma_v$ and $\sigma_h$ are the vertical and horizontal stresses, respectively; $a$ and $b$ are constants related to the material properties. $\sigma_v$ and $\sigma_h$ are used instead of the maximum principal stress $\sigma_1$ and minimum principal stress $\sigma_3$ to distinguish the soil subjected to axial compression and extension loading, respectively.

For representing the in-situ $K_0$-consolidation state, Vaid (1985) modified the hyperbolic model proposed by Duncan and Chang (1970) as

$$q_m=q-q_0=\varepsilon/(1/\overline{E_i}+R_f\times\varepsilon/q_{mf}), \tag{13}$$

where $q$ is the normalized deviator stress $(=(\sigma_v-\sigma_h)/\sigma'_{vc})$; $\sigma'_{vc}$ is the consolidation pressure; $\overline{E_i}$ is the normalized initial tangent Young's modulus; $q_m$ is the increment of normalized deviator stress following consolidation; $q_0$ is the state of zero strain associated with a nonzero end-consolidation normalized deviator stress; and $q_{mf}$ is the failure value of $q_m$.

The normalized tangent Young's modulus $(\overline{E_t})$ can be determined by

$$\overline{E_t}=E_i(1-R_fq_m/q_{mf}). \tag{14}$$

According to Clough and Mana (1976), the ratio of initial Young's modulus over undrained shear strength ($E_i/s_u$) can be assumed to be a constant. The unloading-reloading modulus ($E_{ur}$) is used to simulate both the unloading and reloading conditions. Therefore, only five parameters, i.e., $s_u/\sigma'_v$, $E_i/s_u$, $E_{ur}/s_u$, $R_f$, and $\nu$, are required to fully describe the stress-strain behavior of clay.

### 3.3 Determination of parameters of soil and structure

In the RFEM analysis, the bar element was used to simulate the behavior of the strut. Both the soil and retaining wall were simulated with the eight-node quadrilateral isoparameteric (Q8) elements. The retaining wall and strut were assumed to behave as a linear-elastic material. The geometry of the analysis mesh for RFEM modeling on the Formosa case, as shown in Fig. 4, has 1190 elements and 3654 nodes. Nodes located along sides A and B (Fig. 4) have their horizontal displacement constrained, whereas nodes along side C have all their displacements constrained to simulate a rigid underlying stratum.

The nominal Young's modulus of the diaphragm wall, $E_c$, can be calculated from the suggestion by the American Concrete Institute code (ACI Committee 318, 1995):

$$E_c = 4700\sqrt{f'_c}, \tag{15}$$

where $f'_c$ is the compressive strength of concrete (MPa).

Typically, for an FEM analysis of braced excavation, the nominal $E_c$ is reduced to account for the effect of the underwater construction of the diaphragm wall. Thus, in this study, 80% of the nominal $E_c$ is taken to conduct the RFEM analysis. In the Formosa case, $f'_c$ is equal to 27.44 MPa. The stiffness of struts, $k$, is determined by

$$k = EA / (LS), \tag{16}$$

where $E$ is Young's modulus of steel, $A$ is the cross-sectional area, $L$ is the length, and $S$ is the horizontal span. The stiffness mean values of struts are shown in Table 1. Tables 2 and 3 show the mean values and coefficients of variation (COVs) of soil parameters for each of soil layers. According to Hsiao *et al.* (2008), the mean values of $s_u/\sigma'_v$ and $E_i/s_u$ are found to be 0.30 and 1700 for this case, respectively. The COVs of both $s_u/\sigma'_v$ and $E_i/s_u$ are found to be 0.16. Furthermore, the correlation coefficient between $s_u/\sigma'_v$ and $E_i/s_u$ is adopted to be 0.3. The other parameters shown in Tables 2 and 3 are estimated based on the relevant references with characteristics of soils in the Taipei basin (Cheng, 1987; Moh *et al.*, 1989; Woo and Moh, 1990; Ou *et al.*, 1993; Kung, 2007; Kung *et al.*, 2007a). A constant Poisson's ratio is used in this study due to the difficulty in calibrating its characterization as well as it has a secondary influence on displacement computations (Paice *et al.*, 1996; Fenton and Griffiths, 2002). This study specifies the undrained behavior in clayey layer. In theory, the fully undrained behavior can be obtained with $\nu$=0.5. However, taking $\nu$=0.5 leads to singularity of the stiffness matrix. In order to avoid numerical problems, $\nu$ is taken as 0.49. In addition, $\nu$ is estimated to be 0.3 for sandy layer due to its drained behavior.

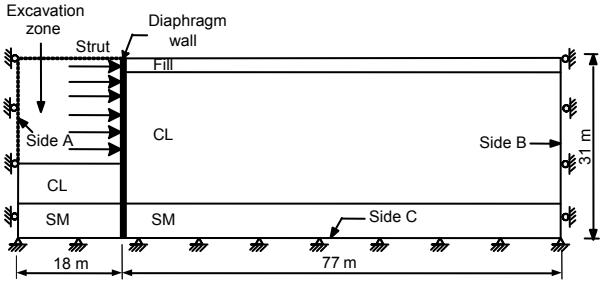


**Fig. 4 Geometry of the Formosa case for RFEM analysis**

**Table 2 Soil parameters for clayey layers used in the RFEM analysis (the pseudo plasticity model)**

| Depth (m) | $\gamma$ (kN/m$^3$) | $s_u$ (kN/m$^2$) | $R_f$ | $E_i/s_u$ | $E_{ur}/s_u$ | $\nu$ |
|---|---|---|---|---|---|---|
| 0.0–2.0 | 18.0 (0.04) | 20 (0.16) | 0.9 (0.11) | 1700 (0.16) | 1700 (0.16) | 0.49 |
| 2.0–25.0 | 18.0 (0.04) | $0.3\sigma'_v$ (0.16) | 0.9 (0.11) | 1700 (0.16) | 1700 (0.16) | 0.49 |

Note: value in () represents the COV of parameter; $\gamma$ represents the moist unit weight of soil

**Table 3 Soil parameters for sandy layers used in the RFEM analysis (the Duncan-Chang model)**

| Depth (m) | $\gamma$ (kN/m$^3$) | $\phi'$ (°) | $R_f$ | $K$ | $K_{ur}$ | $n$ | $\nu$ |
|---|---|---|---|---|---|---|---|
| 25.0–31.0 | 20.0 (0.04) | 33.0 (0.06) | 0.7 (0.11) | 2500 (0.16) | 2500 (0.16) | 0.5 (0.11) | 0.3 |

Note: value in () represents the COV of parameter; $\gamma$ represents the moist unit weight of soil

### 3.4 Examination of FEM analysis of wall deflection

The accuracy of FEM analysis in estimating wall deflection of the Formosa case using the selected soil models and corresponding parameters must be examined first before the RFEM analysis is conducted. Fig. 5 shows the comparison of the wall deflection between field observations and FEM predictions at each excavation stage. Note that FEM analysis was conducted only with the mean value of variables. Overall, the results revealed that the pattern of wall deflection, cantilever type for the first stage, and deep-inward type for later stages, can be appropriately simulated. Also, the calculated maximum wall deflections are very close to the observations at stages 3–7, and the location where the maximum wall deflection occurred is also close to that observed. This reflects that the adopted FEM analysis is capable of capturing the characteristics of deep excavation engineering. However, compared with the results of wall deflection at later stages, the relatively poor agreement of wall deflection at stages 1 and 2 between field observations and FEM prediction is observed. Hsiao *et al.* (2008) indicated that the excavation-induced wall deflection of the first stage, or the first two stages, of excavation is generally different than those of the subsequent stages, which is a well-understood and well-observed phenomenon in a braced excavation. From the practical point of view, the damage to adjacent buildings caused by the excavation in the first two stages is rarely reported, and thus, such discrepancy is considered acceptable. Based on the results, the soil models as well as parameters of soil and structure used for the FEM analysis of wall deflection in the Formosa case are considered adequate and can be employed to conduct the intended RFEM analysis of this case.

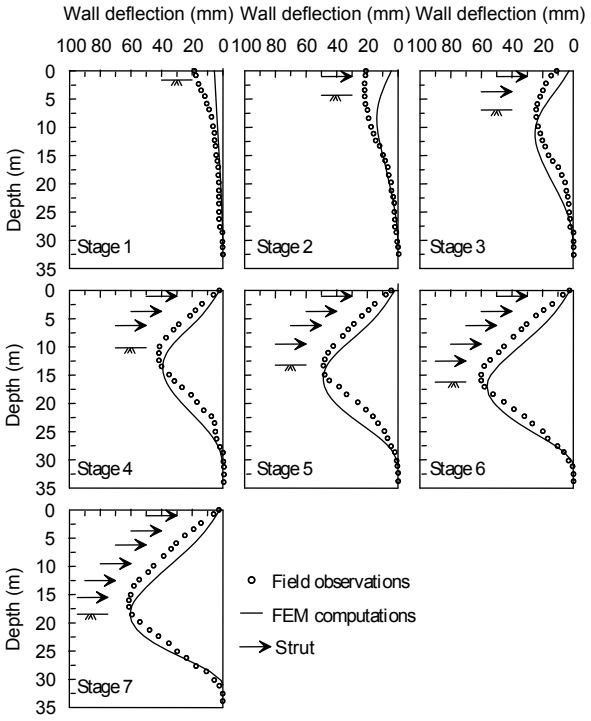


**Fig. 5 Comparison of wall deflection between observations and FEM calculations at each excavation stage**

### 3.5 Considerations of RFEM analysis

It is necessary to determine the probability distributions of input parameters before conducting the RFEM analysis. The lognormal distribution is adopted for all input random variables due to the fact that negative parameter values such as soil strength and stiffness would have no physical meaning. Moreover, the lognormal distribution also appears to perform adequately some statistical characteristics of geotechnical data (Duncan, 2000; Griffiths and Fenton, 2004; Phoon *et al.*, 2006; Wang and Kulhawy, 2008). As a result, the histogram of maximum wall deflection computed by RFEM reveals similar lognormal distributions. The mean value of stiffness of struts and the mean and COVs of soil variables are shown in Tables 1–3, respectively. The COVs of nonsoil variables, including stiffness of struts and the Young's modulus of the diaphragm wall, are specified to be 0.05 based on Hsiao *et al.* (2008).

Since the performance of the RFEM is based on the Monte Carlo simulation, it is important to ensure that the number of simulations is sufficient to provide accurate and stable results. To check this, the Formosa case was analyzed with various numbers of simulations from 100 to 10000. Figs. 6 and 7 show the normalized mean and standard deviation of the maximum wall deflection at various stages with different number of simulations, respectively. Note that the normalized mean of wall deflection is defined as the ratio of mean of wall deflection computed with each of number of simulations over that computed with 10000 simulations. The dash line in Figs. 6 and 7 represent the normalized mean of wall deflection equal 1.0, i.e., the mean of wall deflection with

number of simulation is equal the mean of wall deflection with 10000 simulations. The same definition was adopted for the standard deviation scenario. Based on the analysis results, the mean value and standard deviation of wall deflection will approach a stable value when the number of simulations is greater than 1000. Use of the simulation number of 1000 for RFEM analysis of wall deflection in the Formosa excavation case history is considered appropriate. Hence, the simulation number of 1000 is proposed to conduct the RFEM analysis of excavation.

## 4 Analysis results

The results of RFEM analysis on the Formosa case are shown in Figs. 8–10. As shown in Fig. 8, the relative frequency of occurrence of maximum wall deflection at each of excavation stages is computed. Also the lognormal probability density functions are obtained, which are directly computed using the histogram of the maximum wall deflection. It appears that the theoretical distribution is practically equal to the computed maximum wall deflection. This characteristic accurately reflects the use of lognormal distribution pattern for the input variables.

The analysis results shown in Fig. 8 can be provided to evaluate the probability of exceeding a certain wall deflection. Based on the analysis results, two parameters of the lognormal distributions can be estimated. Then the probability of exceedance, $P_e$, can be easily obtained:

$$P_e = 1 - \Phi\left(\frac{\ln x - \lambda}{\xi}\right), \tag{17}$$

where $\Phi$ denotes the standard normal probabilities; and $\lambda$ and $\xi$ are the parameters of the lognormal distribution, which are the mean and standard deviation of ln$x$, respectively.

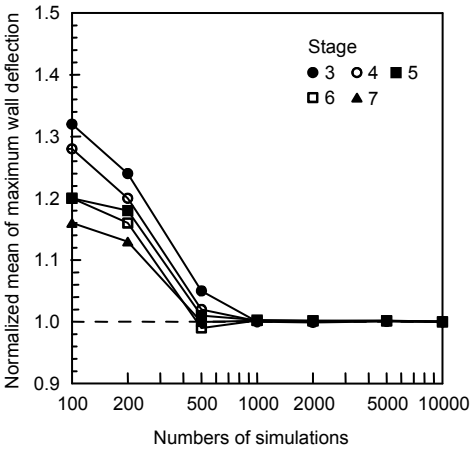


**Fig. 6 The normalized mean value of maximum wall deflection with various simulations**

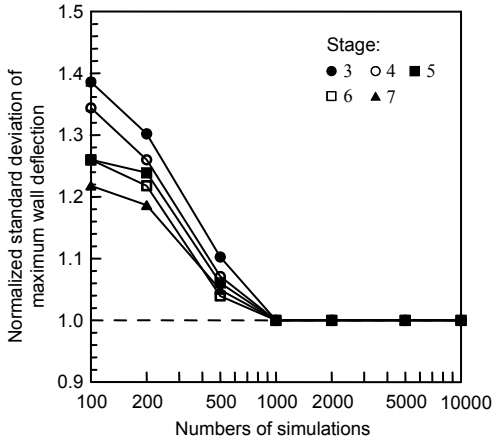


**Fig. 7 The normalized standard deviation of maximum wall deflection with various simulations**

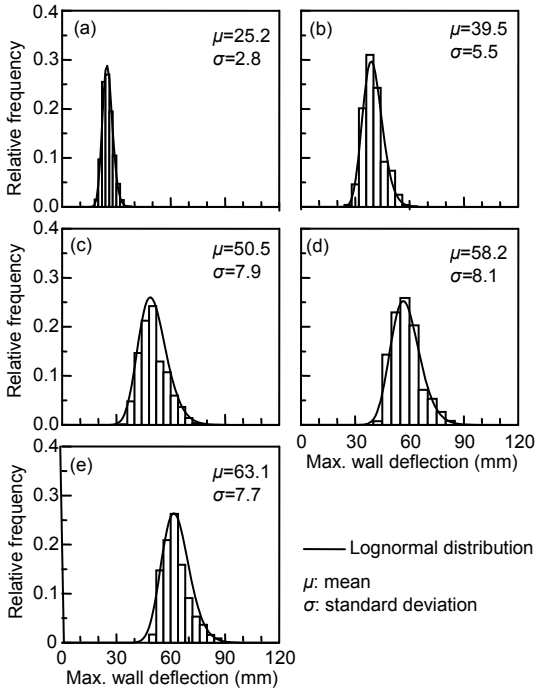


**Fig. 8 Histogram and lognormal distribution of the computed maximum wall deflection**
(a) Stage 3; (b) Stage 4; (c) Stage 5; (d) Stage 6; (e) Stage 7

Fig. 9 displays the probability of exceedance of wall deflections at various excavation stages in the Formosa case, which is a useful chart to evaluate the probability of exceedance a certain wall deflection. For example, if the allowable wall deflection is equal to 60 mm at stage 7, the probability of exceedance is approximately equal to 0.64, which means that the probability of maximum wall deflection greater than 60 mm is 0.64. This chart may provide additional valuable information to engineers for assessing the probability of exceedance of the maximum wall deflection caused by excavation and subsequent the analysis of building damage adjacent to the excavation.

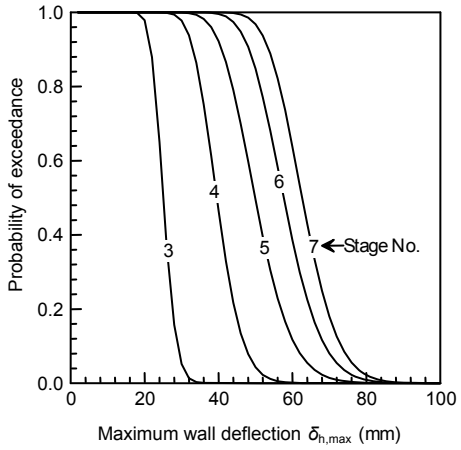


**Fig. 9 The probability of exceedance with respect to various maximum wall deflection**

Finally, this study employed the analysis results to prepare design charts for evaluating the effect of excavation-induced wall deflection on adjacent buildings. In general, the serviceability design of excavation can be performed through the evaluation of damage potential to buildings adjacent to the excavation site. It is recognized that the building damage results from the excavation-induced ground movements, especially the differential settlement. Also, the ground movements are caused by the excavation-induced wall deflection. Therefore, the wall deflection is often adopted as an indicator to evaluate the damage potential of buildings; although, some studies (Son and Cording, 2005; Hsiao *et al.*, 2008; Schuster *et al.*, 2009) have indicated that the use of maximum wall deflection to evaluate the damage potential of adjacent buildings may not be adequate.

When the simplified methods for estimating the wall deflection, ground surface settlement, ground lateral movements, and thus the angular distortion of buildings, are available (Schuster *et al.*, 2009), engineers can perform the task of evaluating the damage potential of buildings based on the estimated maximum wall deflection. Then it becomes feasible to implement the probability analysis of serviceability of adjacent buildings. As shown in Fig. 10, if the allowable maximum wall deflection can be determined first (e.g., 40, 50, 60, 70, or 80 mm), then the probability of exceedance at various excavation stages can be simply obtained based on the results of RFEM analysis of excavation. For example, the allowable value of maximum wall deflection, equal to 60 mm, the probability of exceedance with respect to excavation stages 3–7 are 0.0%, 0.1%, 11.8%, 38.6%, and 63.8%, respectively. For another scenario of $\delta_{h,max}$=70 mm, the probability of exceedance with respect to excavation stages 3–7 are 0.0%, 0.0%, 1.5%, 8.0% and 18.0%, respectively.

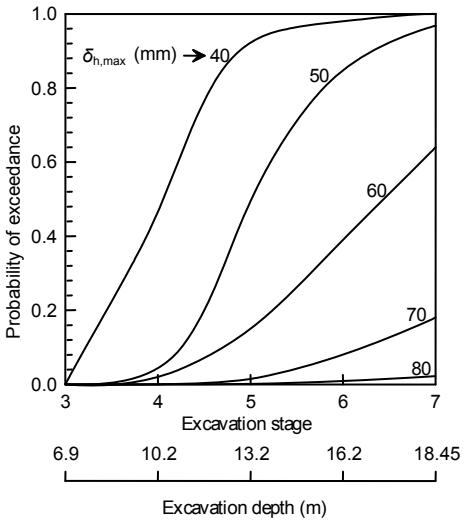


**Fig. 10 The probability of exceedance of allowable maximum wall deflection with respect to various excavation stages**

## 5 Conclusions

This study established a procedure of RFEM analysis for evaluating the probability of exceedance of maximum wall deflection caused by excavation. The RFEM approach involves the Monte Carlo simulation and random variables with joint

probability distributions to consider the uncertainty of input parameters. A well-documented excavation case history is analyzed with the established procedure. According to the results, several conclusions can be drawn.

1. In practice, the number of simulations plays a crucial role in the computation process due to the limited design period and budget. Based on the parametric study, the acceptable number of simulations for the excavation-induced deformation analysis is 1000.

2. Based on the performance of RFEM analysis of wall deflection caused by the Formosa excavation case, the developed RFEM procedure is validated to be an appropriate approach for probability analysis of exceedance of wall deflection. The efficiency of the computation using the developed RFEM approach is satisfactory.

3. The probability of exceedance of maximum wall deflection caused by excavation can be determined through the RFEM analysis. The results showed that the proposed RFEM approach can provide additional probabilistic information to improve the deficiency of conventional FEM for the excavation analysis. In addition, even though the same wall deflection is obtained by the FEM analysis, various levels of risk may be encountered in light of various degrees of uncertainty of the input parameters. The determination of probability of exceedance for maximum wall deflection can be used to practically evaluate the damage potential of buildings adjacent to excavation.

4. A design chart with various allowable maximum wall deflections is provided in this study for evaluating the probability of exceedance of maximum wall deflection at various excavation stages. Although this chart is established based on the Formosa excavation case and may not be applied to another excavation case, it is crucial that this RFEM approach can be applied to establish the design chart for a specific excavation case. Then, the probability analysis of excavation-induced deflection and subsequent damage potential of adjacent buildings becomes feasible.

## References

ACI Committee 318, 1995. Building Code Requirements for Structural Concrete (ACI 318-95) and Commentary (ACI 318R-95). American Concrete Institute (ACI), Farmington Hills, Michigan.

Barry, T.M., 1996. Recommendations on the testing and use of pseudo-random number generators used in Monte Carlo analysis for risk assessment. *Risk Analysis*, **16**(1): 93-105. [doi:10.1111/j.1539-6924.1996.tb01439.x]

Box, G.E., Muller, M.E., 1958. A note on the generation of random normal deviates. *The Annals of Mathematical Statistics*, **29**(2):610-611. [doi:10.1214/aoms/1177706645]

Cheng, T.Y., 1987. Geotechnical Characteristics of Sungshan Formation within Taipei City. MS Thesis, Asian Institute of Technology, Bnagkok.

Clough, G.W., Mana, A.I., 1976. Lessons Learned in Finite Element Analysis of Temporary Excavation in Soft Clay. Desai, C.S. (Ed.), Numerical Method in Geomechanics, Blacksburg, Virginia, p.496-510.

Duncan, J.M., 2000. Factors of safety and reliability in geotechnical engineering. *Journal of Geotechnical and Geoenvironmental Engineering*, **126**(4):307-316. [doi:10.1061/(ASCE)1090-0241(2000)126:4(307)]

Duncan, J.M., Chang, C.Y., 1970. Nonlinear analysis of stress and strain in soils. *Journal of Soil Mechanic Foundation Division*, **96**(5):1629-1651.

Fenton, G.A., Griffiths, D.V., 2002. Probabilistic foundation settlement on spatially random soil. *Journal of Geotechnical Engineering*, **128**(5):381-390. [doi:10.1061/(ASCE)1090-0241(2002)128:5(381)]

Fenton, G.A., Griffiths, D.V., Wiliams, M.B., 2005. Reliability of traditional retaining wall design. *Geotechnique*, **55**(1): 55-62. [doi:10.1680/geot.2005.55.1.55]

Griffiths, D.V., Fenton, G.A., 2001. Bearing capacity of spatially random soil: the undrained clay Prandtl problem revisited. *Geotechnique*, **4**:351-359. [doi:10.1680/geot.51.4.351.39396]

Griffiths, D.V., Fenton, G.A., 2004. Probabilistic slope stability analysis by finite elements. *Journal of Geotechnical and Geoenvironmental Engineering*, **130**(5):507-518. [doi:10.1061/(ASCE)1090-0241(2004) 130:5(507)]

Honjo, M., 2008. Monte Carlo Simulation in Reliability Analysis. Reliability-Based Design in Geotechnical Engineering, Taylor & Francis, London.

Hsiao, E.C.L., Schuster, M., Juang, C.H., Kung, G.T.C., 2008. Reliability analysis and updating of excavation-induced ground surface settlement for building serviceability evaluation. *Journal of Geotechnical and Environmental Engineering*, **134**(10):1448-1458. [doi:10.1061/(ASCE)1090-0241(2008)134:10(1448)]

Hsieh, P.G., Ou, C.Y., 1997. Use of the modified hyperbolic model in excavation analysis under undrained condition. *Geotechnical Engineering Journal*, **28**(2):123-150.

Kondner, R.L., Zelasko, J.S., 1963. A Hyperbolic Stress Strain Formulation for Sands. Proceeding of 2nd Pan-American Conference Soil Mechanics and Foundation Engineering, Brazil, p.289-324.

Kung, G.T.C., 2007. Equipment and testing procedures for small strain triaxial tests. *Journal of the Chinese Institute of Engineers*, **30**(4):579-591. [doi:10.1080/02533839.

2007.9671287]

Kung, G.T.C., Hsiao, E.C.L., Juang, C.H., 2007a. Evaluation of a simplified small-strain soil model for estimation of excavation-induced movements. *Canadian Geotechnical Journal*, **44**(6):726-736. [doi:10.1139/t07-014]

Kung, G.T.C., Juang, C.H., Hsiao, E.C.L., Hashash, Y.M.A., 2007b. Simplified model for wall deflection and ground-surface settlement caused by braced excavation in clays. *Journal of Geotechnical and Geoenvironmental Engineering*. **133**(6):731-747. [doi:10.1061/(ASCE)1090-0241(2007)133:6(731)]

Kung, G.T.C., Ou, C.Y., Juang, C.H., 2009. Modeling small-strain behaviour of Taipei clays for finite element analysis of braced excavations. *Computers and Geotechnics*, **36**(1-2):304-319. [doi:10.1016/j.compgeo.2008.01.007]

Moh, Z.C., Chin, C.T., Liu, C.J., Woo, S.M., 1989. Engineering correlations for soil deposits in Taipei. *Journal of the Chinese Institute of Engineers*. **12**(3):273-283.

Ou, C.Y., Hsieh, P.G., Chiou, D.C., 1993. Characteristics of ground surface settlement during excavation. *Canadian Geotechnical Journal*, **30**(5):758-767. [doi:10.1139/t93-068]

Paice, G.M., Griffiths, D.V., Fenton, G.A., 1996. Finite element modeling of settlements on spatially random soil. *Journal of Geotechnical Engineering*, **122**(9):777-779. [doi:10.1061/(ASCE)0733-9410(1996)122:9(777)]

Phoon, K.K., Chen, J.R., Kulhawy, F.H., 2006. Characterization of Model Uncertainties for Augered Cast-in-Place (ACIP) Piles under Axial Compression. Proc. Foundation Analysis and Design: Innovative Methods (GSP 153), Shanghai, p.82-89.

Schuster, M., Kung, G.T.C., Juang, C.H., Hashash, Y.M.A., 2009. Simplified model for evaluating damage potential of buildings adjacent to a braced excavation. *Journal of Geotechnical and Geoenvironmental Engineering*, **135**(12):1823-1835. [doi:10.1061/(ASCE)GT.1943-5606.0000161]

Son, M., Cording, E.J., 2005. Estimation of building damage due to excavation-induced ground movements. *Journal of Geotechnical Geoenvironmental Engineering*, **131**(2):162-177. [doi:10.1061/(ASCE)1090-0241(2005)131:2(162)]

Vaid, Y.P., 1985. Effect of consolidation history and stress path on hyperbolic stress-strain relations. *Canadian Geotechnical Journal*, **22**(2):172-176. [doi:10.1139/t85-024]

Wang, Y., Kulhawy, F.H., 2008. Reliability index for serviceability limit state of building foundations. *Journal of Geotechnical and Geoenvironmental Engineering*, **134**(11):1587-1594. [doi:10.1061/(ASCE)1090-0241(2008)134:11(1587)]

Woo, S.M., Moh, Z.C., 1990. Geotechnical Characteristics of Soil in the Taipei Basin. Tenth Southeast Asian Geotechnical Conference, Taipei, p.51-65.

## 2010 JCR of Thomson Reuters for *JZUS-A* and *JZUS-B*

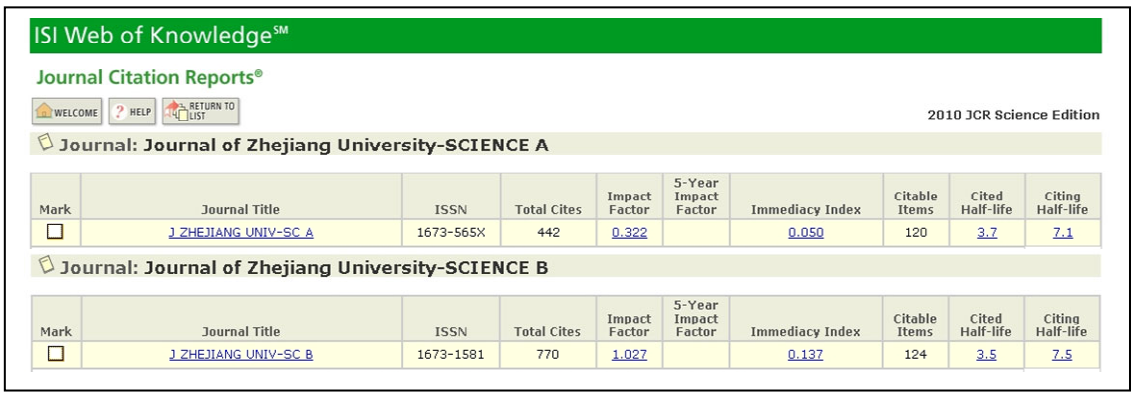

ISI Web of Knowledge℠

Journal Citation Reports®

WELCOME | HELP | RETURN TO LIST

2010 JCR Science Edition

Journal: Journal of Zhejiang University-SCIENCE A

| Mark | Journal Title | ISSN | Total Cites | Impact Factor | 5-Year Impact Factor | Immediacy Index | Citable Items | Cited Half-life | Citing Half-life |
|---|---|---|---|---|---|---|---|---|---|
| ☐ | J ZHEJIANG UNIV-SC A | 1673-565X | 442 | 0.322 | | 0.050 | 120 | 3.7 | 7.1 |

Journal: Journal of Zhejiang University-SCIENCE B

| Mark | Journal Title | ISSN | Total Cites | Impact Factor | 5-Year Impact Factor | Immediacy Index | Citable Items | Cited Half-life | Citing Half-life |
|---|---|---|---|---|---|---|---|---|---|
| ☐ | J ZHEJIANG UNIV-SC B | 1673-1581 | 770 | 1.027 | | 0.137 | 124 | 3.5 | 7.5 |